Journal of Alloys and Compounds 523 (2012) 146–150

Contents lists available at SciVerse ScienceDirect

Journal of Alloys and Compounds

journal homepage: www.elsevier.com/locate/jallcom

# Size-dependent flowing characteristics of a Zr-based bulk metallic glass in the supercooled liquid region

N. Li*, D.J. Li, X.Y. Wang, L. Liu

*State Key Lab for Materials Processing and Die & Mould Technology, and College of Materials Science and Engineering, Huazhong University of Science and Technology, 430074 Wuhan, People's Republic of China*

ARTICLE INFO

*Article history:*
Received 20 December 2011
Received in revised form 18 January 2012
Accepted 23 January 2012
Available online 2 February 2012

*Keywords:*
Bulk metallic glass
Flowing characteristics
Size-dependent
Weibull statistics

ABSTRACT

The flowing characteristics of a Zr-based bulk metallic glass (BMG) with different diameters but the same aspect ratio was investigated through uniaxial compression in the supercooled liquid region. The compressive stress increases with decreasing sample dimension at various strain rates, the corresponding strain rate sensitivity ($m$) was calculated and a deformation map that describes the size-dependent transition from Newtonian to non-Newtonian flow was constructed. The size-dependent flowing characteristics can be rationalized using the Weibull statistics with a Weibull modulus of 27.4. Finite element analysis showed that the friction between the jigs and the specimen induces different stress distributions among the specimens under uniaxial compression, which is responsible for the size-dependent flowing characteristics.



## 1. Introduction

Bulk metallic glasses (BMGs) have enduring attractions due to their impressive properties, including extraordinary strength and hardness, relatively high fracture toughness, good soft magnetic properties, excellent corrosion and wear resistance [1,2]. In particular, BMGs have the capability to superplastic flow in the supercooled liquid region, showing superior formability and good geometrical transferability, such unique characteristic has been widely utilized for thermoplastic microforming [3,4].

While at micron or submicron scale, the size-dependent deformation behavior has been widely observed in BMGs at room temperature. For example, Guo et al. [5] found the large tensile ductility in the range of 23–45% when the dimension of monolithic metallic-glass samples decreases down to the order of 100 nm, and interpreted the phenomenon from the driving force perspective. The size dependent compressive plasticity has also been reported in other lectures, and a few theories or models have been proposed, such as the plastic zone size theory [6], free volume adiabatic heating model [7,8], stiffness effect of the testing machine [9] and intermittent sliding model [10]. On the other hand, Lee et al. [11] observed that the average yield strength of the micron-scaled pillars (range from 1342 to 1580 MPa) is much higher than that for the millimeter-scaled samples (about 800 MPa), demonstrating a strong sample size effect. However, BMGs exhibit the homogeneous flow characteristics in the supercooled liquid region, where each volume element of the specimen contributes to the strain. This homogeneous flow can be divided into two different deformation modes, viz. Newtonian and non-Newtonian flow modes [12,13], and the transition from Newtonian to non-Newtonian flow is strongly dependent on the testing temperature and strain rate in addition to other factors such as forming time, stress state and alloy systems [14–16]. This homogeneous flow characteristic has been demonstrated very important for the microforming of BMGs [4,17].

Accordingly, it is worth noting that the influence of decreasing sample size on the flowing characteristic of BMGs near or in the supercooled liquid region, which is particularly important from the viewpoint of micro-processing and application of BMGs. However, to the best of our knowledge, the size-dependent flowing characteristic of BMGs in the supercooled liquid region has rarely been reported. In the present work, uniaxial compressive tests of $Zr_{65}Cu_{17.5}Ni_{10}Al_{7.5}$ BMGs with different sample sizes were performed in the supercooled liquid region. The underlying mechanism for the size-dependent flowing characteristic is analyzed via the Weibull statistics and finite element method (FEM).

## 2. Experimental procedure

The $Zr_{65}Cu_{17.5}Ni_{10}Al_{7.5}$ (atomic ratio) bulk metallic glass with diameter of 4 mm and length of 100 mm was fabricated by arc-melting a mixture of pure Zr, Cu, Ni, and Al metals (purity >99.5%) under a Ti-gettered argon atmosphere, followed by drop casting into cooper molds. To minimize the initial free volume difference among different sized samples caused by different cooling rates during solidification, other size cylindrical specimens (Ø 1–3 mm) were precision machined under water cooling from the as-cast Ø 4 mm rod [8], and polished through 3000 grit SiC paper. The structures of the samples obtained were examined by X-ray diffraction (*XRD*, Philips $\chi$' Pert PRO). The thermal response of all alloys was investigated with

* Corresponding author. Tel.: +86 27 87556894; fax: +86 27 87554405.
*E-mail address:* hslining@mail.hust.edu.cn (N. Li).

0925-8388/$ – see front matter © 2012 Elsevier B.V. All rights reserved.
doi:10.1016/j.jallcom.2012.01.136

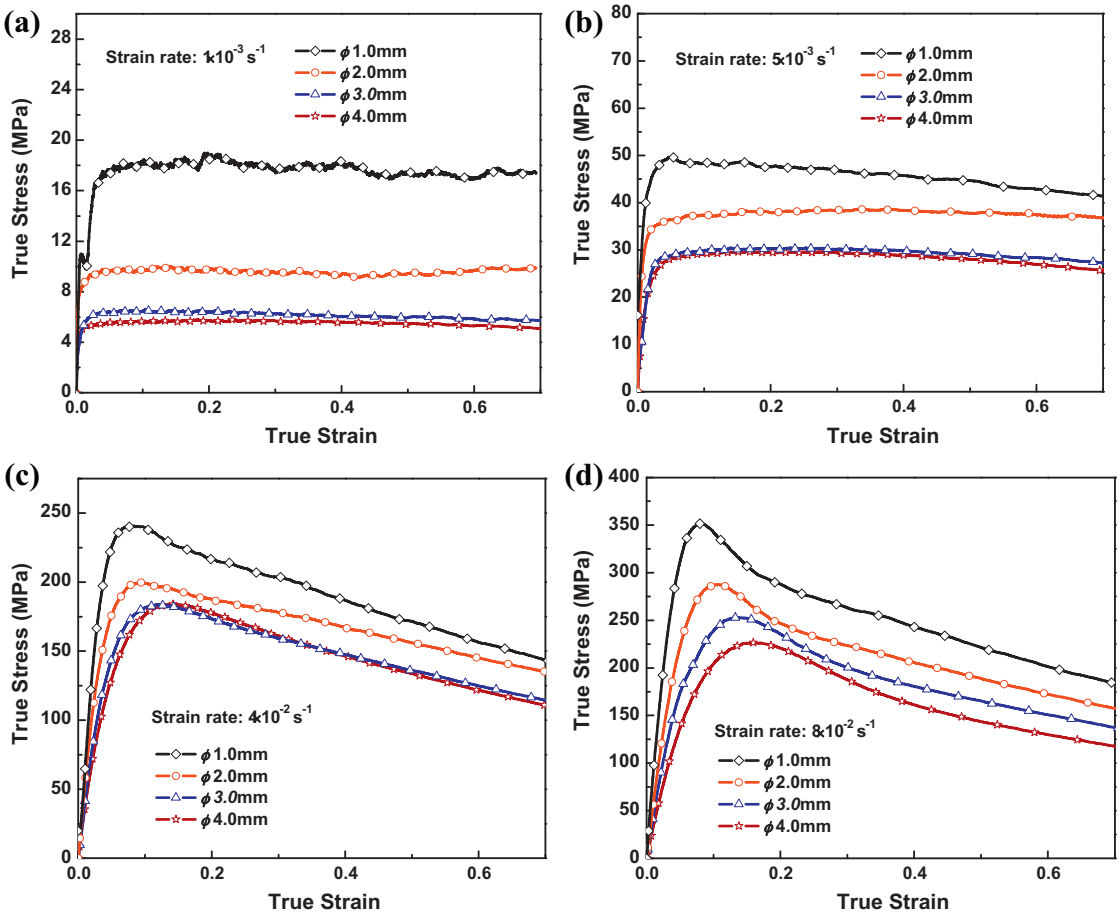


**Fig. 1.** The compressive true stress–strains for Zr-based BMGs with different diameters at various strain rates: (a) $1 \times 10^{-3}$ s$^{-1}$; (b) $5 \times 10^{-3}$ s$^{-1}$; (c) $4 \times 10^{-2}$ s$^{-1}$; (d) $8 \times 10^{-2}$ s$^{-1}$.

differential scanning calorimetry (*DSC*, Perkin–Elmer DSC-7) at a heating rate of 20 K/min in a flow of argon, which revealed that all samples with different diameters exhibit almost identical thermal behavior with a distinct glass transition temperature ($T_g$) of 363 °C and a wide supercooled liquid region of 107 °C. The incubation time for crystallization at various temperatures was measured using DSC in an isothermal mode, which revealed that the incubation time is around 180 min at 400 °C.

The compression specimens with normal aspect ratio of 1.33 were cut from the corresponding cylindrical rods (Ø 1–4 mm) using a diamond blade under water cooling. Two ends of the specimens were polished carefully to ensure that they are parallel each other and are perpendicular to the longitudinal axis of the sample. Uniaxial compression tests were conducted at 400 °C (~$1.1T_g$) at various strain rates (ranging from $1 \times 10^{-3}$ s$^{-1}$ to $8 \times 10^{-2}$ s$^{-1}$) using a Zwick machine (Zwick/Roell 020) equipped with an air furnace. Graphite lubricant was used to reduce the friction at the die-specimen interface. In order to shorten the time for heating the specimen, the load train was preheated to the test temperature and held for 30 min to stabilize the temperature. The specimen was then placed promptly into the load train with a holding time of 2 min. All the specimens were subjected to a total plastic strain of 40% and air cooled after the tests. To investigate the stress-induced microstructure evolution, the stress distribution of deformed specimens was simulated using commercially available DEFORD-3D software.

## 3. Results

Fig. 1 shows the true stress–true strain ($\sigma - \varepsilon$) curves of the $Zr_{65}Cu_{17.5}Ni_{10}Al_{7.5}$ BMG with different diameters at a certain temperature (400 °C, ~$1.1T_g$) but various strain rates. It is evident that the deformation behavior is not only dependent on the strain rate, but also sensitive to the sample diameter. The flow stress increases with increasing strain rate, as described in Fig. 1(a)–(d), similar to that reported in many other BMGs [18,19]. However, at a certain strain rate, the flow stress increases with the decrease of the sample dimension. For example, at a strain rate of $1 \times 10^{-3}$ s$^{-1}$ (see Fig. 1a), the steady flow stress ($\sigma_{flow}$) is only 5.6 MPa for the specimen with the largest diameter of 4 mm, while $\sigma_{flow}$ increases up to about 8.7 MPa when the diameter of the specimen decreases to 2 mm, and this tendency becomes more prominent for the specimen with the smallest diameter of 1 mm, which exhibits the largest flow stress of about 18 MPa. The similar phenomenon can also be observed at higher strain rates, i.e. $5 \times 10^{-3}$ s$^{-1}$ to $8 \times 10^{-2}$ s$^{-1}$ (see Fig. 1(b)–(d)), indicating a strong size-dependent deformation behavior. $\sigma - \varepsilon$ curves for specimens with different diameters, on the other hand, are characterized by monotonous increase of flow stress in the initial stage of deformation, followed by steady-state flow with stress plateau in the extended strain region at low strain rate range, i.e. from $1 \times 10^{-3}$ s$^{-1}$ to $5 \times 10^{-3}$ s$^{-1}$ (see Fig. 1(a) and (b)). It is interesting that at the strain rate of $5 \times 10^{-3}$ s$^{-1}$, the $\sigma - \dot{\varepsilon}$ curve of the specimen with the smallest diameter of 1 mm exhibits a distinct stress overshoot. With increasing strain rate, the stress overshoot was happened at all specimens, but the height of the stress overshoot is larger for the sample with smaller diameter at a certain strain rate (such as $4 \times 10^{-2}$ s$^{-1}$ or $8 \times 10^{-2}$ s$^{-1}$, see Fig. 1(c) and (d)).

Fig. 2(a) presents the logarithmic relationship between the nominal flow stress and the strain rate for the $Zr_{65}Cu_{17.5}Ni_{10}Al_{7.5}$ BMG with different diameters under uniaxial compression at a temperature of 400 °C (~$1.1T_g$). It can be seen clearly that the flow stress increased monotonously with the increase of strain rate for all samples with different dimensions. However, the flexion at each curve is different from each other, which is located at $\dot{\varepsilon} = 5 \times 10^{-3}$ s$^{-1}$ for the specimen with diameter of 1 mm, $1 \times 10^{-2}$ s$^{-1}$ for the Ø 2 mm, and $4 \times 10^{-2}$ s$^{-1}$ for the Ø 3–4 mm samples. The data blow the flexions can be well fitted by a straight line with a slope of about 1,

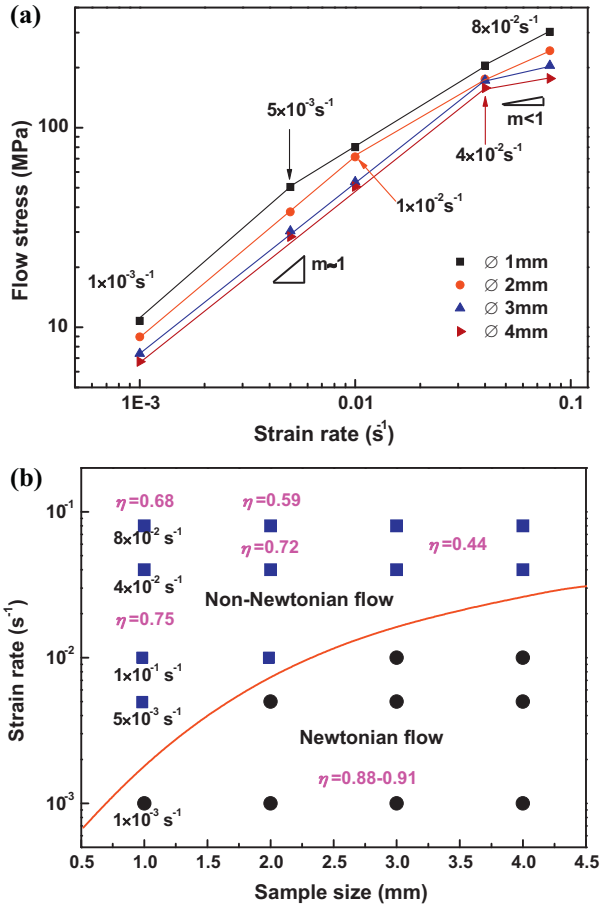


**Fig. 2.** For the Zr-based BMGs with different diameters: (a) the logarithmic relationship between the flow stress and the strain rate; (b) deformation map with power dissipation efficiency distribution.

this slope actually reflects the values of the strain rate sensitivity ($m$) according to the definition of $m = \partial \log \sigma_{flow}/\partial \log \dot{\varepsilon}$ [20]. The value of $m$ is very close to unity before the flexion at low strain rate regime, indicating that the deformation of the BMG behaves nearly in a Newtonian flow. However, $m$ decreases down to below 1 with increasing strain rate, indicating a transition from Newtonian to non-Newtonian flow.

According to the values of $m$ for all specimens with different dimensions, a deformation map is constructed and presented in Fig. 2(b), where the sample size ranging from Ø 1 to 4 mm and the strain rate ranging from $1 \times 10^{-3}\ s^{-1}$ to $8 \times 10^{-2}\ s^{-1}$. Over this range, two distinct regimes of flow character can be observed, i.e., Newtonian and non-Newtonian flow. From Fig. 2(b), it can be seen clearly that the flowing characteristics is closely related to the sample dimension at the low strain rate regime ($\dot{\varepsilon} < 4 \times 10^{-2}\ s^{-1}$), i.e. the transition from Newtonian to non-Newtonian flow would occur easier in the sample with smaller diameter.

## 4. Discussion

The transition from Newtonian to non-Newtonian flow can be analyzed in the framework of Weibull statistics [21,22]. The Weibull equation describes the transition probability $P_f$ as a function of a given compressive flow stress ($\sigma_{trans}$) at critical strain rate (in which the transition happens) in form of

$$P_f = 1 - \exp\left[-V\left(\frac{\sigma_{trans} - \sigma_u}{\sigma_0}\right)^n\right] \quad (1)$$

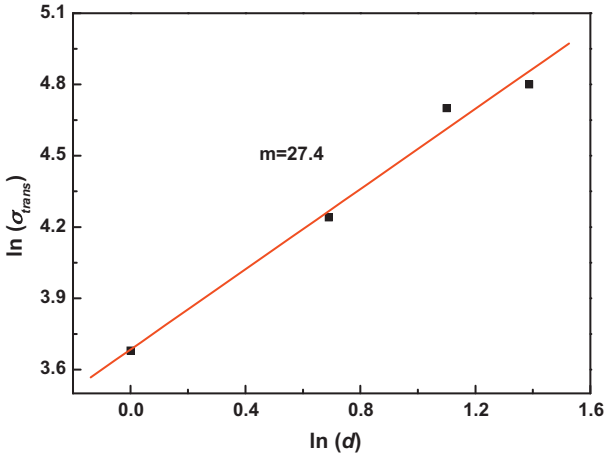


**Fig. 3.** The logarithmic relationship between flow stress (in which the transition from Newtonian to non-Newtonian happened) and sample diameter.

where $\sigma_0$ is a scaling parameter, $n$ is the Weibull modulus and $V$ is the volume of the tested sample, the parameter $\sigma_u$ denotes the stress at which there is a zero transition probability, which is usually taken to be zero. Assume the characteristic viscous flow causing transition in all samples are the same, then, at a fixed transition probability, i.e. $P_f$ is constant, Eq. (1) reduces to

$$V\left(\frac{\sigma_{trans}}{\sigma_0}\right)^n = const \quad (2)$$

For the specimens with different diameters, $d$, Eq. (2) can be rewritten as

$$d^3\sigma_{trans}^n = const \quad (3)$$

Plot of transition flow stress at critical strain rate versus sample diameter for the Zr-based BMGs is described in Fig. 3. In the investigated dimension range, the linear correlation between ln $\sigma_{trans}$ and ln $d$ indicates that the size-dependent transition from Newtonian to non-Newtonian flowing characteristics can be well described by the Weibull distribution with a high Weibull modulus $n = 27.4$.

In general, for the BMGs deformed in the supercooled liquid region, the softening mechanism is mainly controlled by thermal process, resulting in indifference in flowing stress and free volume creation [23]. Nevertheless, in studying the compressive deformation of Pd-based bulk metallic glass, Kim et al. [24,25] reported that the local deformation within the specimen is heterogeneous due to some non-linear factors such as the friction between the specimen and the die surfaces, which induce local stress concentration. In order to investigate the local deformation states in the specimens with different diameters in the present work, the compressive processes of Zr-based BMGs with different diameters are simulated by commercial software *DEFORM 3D*. A Maxwell constitutive model that we proposed [26] is defined using the data from our own compressive test at various strain rates. The simulated distribution of the effective stress at true strain $\varepsilon = 0.7$ was obtained, and the typical samples with the smallest diameter of 1 mm and the largest diameter of 4 mm was selected. The simulated distributions of the effective stress at cross section are described in Fig. 4. From Fig. 4(a), the compressive stress concentrates at strain rate of $1 \times 10^{-3}\ s^{-1}$ most heavily in the edge and center regions, indicating a prominent heterogeneous deformation locally. This phenomenon can also be observed at higher strain rate of $8 \times 10^{-2}\ s^{-1}$ (see Fig. 4(c)), in consistent with what reported by Jun et al. who attributed it to the friction between the jigs and the specimen [25]. However, this compressive stress concentration becomes mild for the specimen with diameter of 4 mm at all

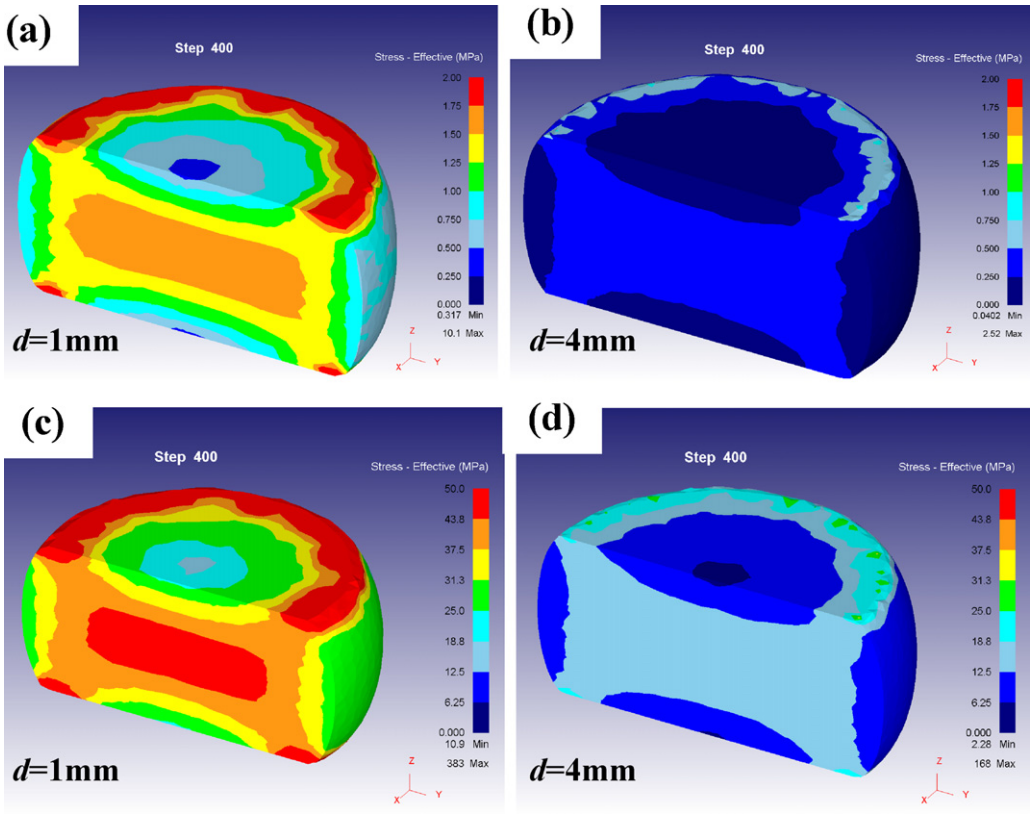


**Fig. 4.** Simulated stress distribution in specimens with different diameters under strain rates of (a) and (b) $1 \times 10^{-3}$ s$^{-1}$; (c) and (d) $8 \times 10^{-2}$ s$^{-1}$.

strain rates, as described in Fig. 4(b) and (d), respectively. The stress distribution in specimens has been reported induce diversity of free volume distribution [25], which may responsible for the size-dependent transition from Newtonian to non-Newtonian flowing characteristic.

The friction between the jigs and the specimen during the uniaxial compression dissipates energy, which would result in different viscous flow and can be interpreted by the power dissipation efficiency based on the dynamic materials model (DMM) proposed by Prasad et al. [27]. According to the DMM model, the total amount of power consumption during a hot deformation process is viewed here to consist of the two complementary functions, viz. the $G$ content representing heat dissipation and the $J$ co-content used for a structural rearrangement. The structural rearrangement is in general more effective than a thermal dissipation for a dynamic softening during a hot forming process, so that a higher forming efficiency can be achieved for a larger value of $J$. The power dissipation efficiency $\eta$ was defined as,

$$\eta = \frac{J}{J_{\max}} = \frac{2m}{m+1} \tag{4}$$

where the parameter $m$ denoting the strain rate sensitivity. The values of $\eta$ for different size samples at various strain rates were then calculated and the distribution of $\eta$ was described in Fig. 2(b). It can be seen clearly that the high value of $\eta$ ranging from 0.88 to 0.91 is located in the Newtonian flow region [28], indicates that the input energy can be used most effectively for the viscous flow with the least thermal dissipation, especially for the specimens with larger diameters which exhibits more homogeneous deformation with lower flow stress.

## 5. Conclusions

In summary, the flowing characteristics of $Zr_{65}Cu_{17.5}Ni_{10}Al_{7.5}$ BMG with different diameters was investigated in the supercooled liquid region under uniaxial compression.

(1) The flow stress increases with decreasing specimen diameter, and a deformation map that describes the size-dependent transition from Newtonian to non-Newtonian behavior was constructed.
(2) The size dependent flowing characteristic can be rationalized using the Weibull statistics.
(3) The friction between the cylindrical workpiece and the die produces different stress distribution, which results in different viscous flow that can be described by power dissipation efficiency model. This friction effect responsible for size-dependent flowing characteristic for the BMGs deformed in the supercooled liquid region.

## Acknowledgements

This work was financially supported by the National Nature Science Foundation of China under Grant No 51005081, 51175202 and 973 program under Grant No 2007CB613908. The work was also partially supported by the fund of the State Key Laboratory of Solidification Processing in NWPU. The authors are grateful to the Analytical and Testing Center, Huazhong University of Science and Technology for technical assistance.

## References

[1] A. Inoue, Acta Mater. 48 (2000) 279–306.
[2] W.L. Johnson, MRS Bull. 24 (1999) 42–56.

[3] G. Kumar, H. Tang, J. Schroers, Nature 457 (2009) 868–872.
[4] J. Schroers, Adv. Mater. 21 (2009) 1–32.
[5] H. Guo, P.F. Yan, Y.B. Wang, J. Tan, Z.F. Zhang, M.L. Sui, E. Ma, Nat. Mater. 6 (2007) 735–739.
[6] M.F. Ashby, A.L. Greer, Scripta Mater. 54 (2006) 321–326.
[7] Y.J. Huang, J. Shen, J.F. Sun, Appl. Phys. Lett. 90 (2007) 081919.
[8] N. Li, Q. Chen, L. Liu, J. Alloys Compd. 493 (2010) 142–147.
[9] Z. Han, W.F. Wu, Y. Li, Y.J. Wei, H.J. Gao, Acta Mater. 57 (2009) 1367–1372.
[10] S.X Song, H. Bei, J. Wadsworth, T.G. Nieh, Intermetallics 16 (2008) 813–818.
[11] C.J. Lee, J.C. Huang, T.G. Nieh, Appl. Phys. Lett. 91 (2007) 161913.
[12] T.G. Nieh, J. Wadsworth, C.T. Liu, T. Ohkubo, Y. Hirotsu, Acta Mater. 49 (2001) 2887–2896.
[13] H. Kato, Y. Kawamura, A. Inoue, H.S. Chen, Appl. Phys. Lett. 73 (1998) 3665.
[14] Y. Kawamura, T. Nakamura, A. Inoue, T. Masumoto, Mater Trans., JIM. 40 (1999) 794–803.
[15] Y. Kawamura, T. Nakamura, H. Kato, H. Mano, A. Inoue, Mater. Sci. Eng. A 304–306 (2001) 674–678.
[16] Y. Kawamura, A. Inoue, Appl. Phys. Lett. 77 (2000) 1114.
[17] K.S. Lee, H.J. Jun, Y.W. Chang, Mater. Sci. Eng. A 449-451 (2007) 941–944.
[18] Y. Kawamura, T. Shibata, A. Inoue, T. Masumoto, Appl. Phys. Lett. 69 (1996) 1208.
[19] T.G. Nieh, J. Wadsworth, Scripta Mater. 54 (2006) 387–392.
[20] Y. Kawamura, T. Nakamura, A. Inoue, Scripta Mater. 39 (1998) 301–306.
[21] W. Weibull, J. Appl. Mech. 18 (1951) 293–297.
[22] L. Velázquez-Ortega, S. Rodríguez-Romo, Chem. Eng. Sci. 64 (2009) 2866–2880.
[23] N. Li, L. Liu, K.C. Chan, Q. Chen, J. Pan. Intermetallics. 17 (2009) 227–230.
[24] H.S. Kim, H. Kato, A. Inoue, H.S. Chen, Acta Mater. 52 (2004) 3813–3823.
[25] H-J. Jun, K.S. Lee, S.C. Yoon, H.S. Kim, Y.W. Chang, Acta Mater. 58 (2010) 4267–4280.
[26] X.Y. Wang, N. Tang, Z.Z. Zheng, Y.Y. Tang, J.J. Li, L. Liu, J. Alloys Compd. 509 (2011) 2518–2522.
[27] Y.V.R.K. Prasad, H.L. Gegel, S.M. Doraivelu, J.C. Malas, J.T. Morgan, K.A. Lark, D.R. Barker, Metal. Trans. 15A (1984) 1883.
[28] J.N. Mei, J.L. Soubeyroux, J.J. Blandin, J.S. Li, H.C. Kou, H.Z. Fu, L. Zhou, Intermetallics 19 (2011) 48–53.